Supplemental Material

Estimation of Size and Contact Angle of Evaporating Sessile Liquid Drops Using Texture Analysis

Chonghua Xue, Jared T. Lott, Vijaya B. Kolachalama

1 GUI Development

We developed a free, user-friendly software that can estimate the drop diameter using the modified HCD approach and contact angle using the Gabor wavelet-based approach. The standalone software application was developed using MATLAB 2018a (Mathworks Inc., Natick, MA). The logical workflow of the software is intuitive and straightforward (**Figure S2**). It takes in a single image or a video as input, and after a few essential initialization steps, the results can be generated and presented in an organized format. Additionally, all results can be saved in '.mat' format for further analysis. To make this software easy to use, we have optimized certain parameters that are now part of the default GUI settings. These settings should allow the users to obtain results for most scenarios without spending too much time to adjust the parameters. However, full flexibility is granted in order to handle any complex cases. For example, all parameters such as Gabor wavelet functions and optimization settings can be manipulated to serve any specific need. Moreover, the manipulation is facilitated by a set of graphs that help users to find the ideal settings with minimal effort.

2 Optimization Methods

Optimization is required during aligning the Gabor wavelet to the drop edge. We implemented three methods (gradient ascent, Newton's method and hybrid method) that might satisfy the needs for this problem.

2.1 Gradient ascent algorithm

Gradient ascent is a first-order iterative optimization algorithm for finding the optimum of a function. It has been widely applied in numerous contexts due to its simplicity and robustness. We therefore use gradient ascent to fit the Gabor wavelet. Let's denote the overall response as a function of θ and d.

$$f(\theta, d) = \sum_{x,y} G_{\theta,d}[x, y] \cdot I[x, y] \tag{A.1}$$

For iteration t and progress step η, we have

$$[\theta_{t+1}, d_{t+1}]^T = [\theta_t, d_t]^T + \eta \cdot \nabla_{\theta,d} f(\theta_t, d_t), \quad t = 0, 1, 2, \ldots \tag{A.2}$$

With stop criterion $\epsilon > 0$, the algorithm terminates when

$$\left| f(\theta_{t+1}, d_{t+1}) - f(\theta_t, d_t) \right| < \epsilon \tag{A.3}$$

The gradient $\nabla_{\theta,d} f(\theta_t, d_t)$ is numerically approximated by the difference quotient

$$\nabla_{\theta,d} f(\theta_t, d_t) \approx \Big[\frac{f(\theta_t + \delta, d_t) - f(\theta_t - \delta, d_t)}{2\delta}, \frac{f(\theta_t, d_t + \delta) - f(\theta_t, d_t - \delta)}{2\delta} \Big]^T \tag{A.4}$$

Note that $\nabla_{\theta,d} f(\theta_t, d_t)$ has a closed form expression, but it was proved to be computationally more expensive in our experiment. So, we turned to numerical approximation which yields comparable precision at a faster rate.

2.2 Other optimization methods

We also implemented Newton's method which leveraged both the first-order and the second-order derivatives to locate the extremum of a function. The contour map (**Figure 4B**) shows that the local area around the optimum is flat with respect to one direction, but steep with respect to the other. For gradient-based method, optimization on such 'ridge-like' area is challenging since large progress step η will lead to overshooting while small η will instead slow down the convergence process. Newton's method, therefore, is a good alternative for speeding up the optimization, especially when the target function is reasonably well-behaved in terms of concavity and smoothness.

The downside of Newton's method is that it is very sensitive to local convexity/concavity, making itself vulnerable to any type of extrema. Namely, an improper initialization will easily lead to an unwanted result. Thus, we proposed a hybrid approach as a trade-off between the robustness of gradient ascent and the speed of Newton's method. Given θ_0 and d_0, the optimization starts with gradient ascent which will bring θ and d sufficiently close to maximum. This can be achieved by setting a loose stop criterion so that gradient ascent will stop early. Then, Newton's method takes over and continues with finer stop criterion. In our experiment, the computational efficiency of the hybrid approach was comparable to Newton's method, but without a precise initialization of θ and d.

3 Analysis of Reflection Generated Error

As the Gabor wavelet is placed at the contact point, the reflection profile may perturb the measurement accuracy. An issue arises during the optimization as the Gabor wavelet is not only trying to align with the true edge, but also with the reflected edge. It is important to thoroughly understand the correspondence between the reflected profile and the error. We established a theoretical analysis to define a closed form expression of the error, followed by a numerical simulation to identify the regions of interest with minimal error.

3.1 Problem formulation

Let $I_\alpha(x, y)$ signify the region of interest where the rotation of the reflected edge is α.

$$I_\alpha(x,y) = \begin{cases} -c, & (x,y) \in \Omega_D \\ 0, & (x,y) \in \Omega_B \end{cases} \tag{A.5}$$

Now, let $R_\alpha(\theta)$ denote the overall response. It is a function of θ depending on the reflected edge rotation α. Here Ω_D is the area of the drop profile and Ω_B is the area of the background (**Figure S6**).

$$\begin{aligned} R_\alpha(\theta) &= \iint_\Omega G_\theta(x,y)\, I_\alpha(x,y)\, dxdy = -c \iint_{\Omega_D} G_\theta(x,y)\, dxdy \\ &= -c \int_0^\infty dx \int_{x\tan\alpha}^\infty G_\theta(x,y)\, dy. \end{aligned} \tag{A.6}$$

As to the definition of the Gabor wavelet function $G_\theta(x,y)$, please refer to **Equation 8**. Also, let θ_α^* be the optimum of the following optimization:

$$\theta_\alpha^* = \arg\max_\theta R_\alpha(\theta). \tag{A.7}$$

If the Gabor wavelet is perfectly aligned with the true edge which is vertical, the corresponding θ becomes exactly 0. Therefore, the measurement error ϵ_α with respect to α is

$$\epsilon_\alpha = \theta_\alpha^* - 0 = \arg\max_\theta R_\alpha(\theta). \tag{A.8}$$

3.2 Simulation on synthetic images

It is important to understand how ϵ_α varies with respect to α. The analytical form of ϵ_α, however, is hard to derive except for $\alpha = 0$ (**Equation A.14**). Moreover, Taylor expansion approximation is more likely to fail when α approaches -90° or 90°. Therefore, we performed a numerical simulation to account for all the scenarios.

Drop images were synthetically generated based on $I_\alpha(x,y)$ (**Equation A.5**). By iterating α from -90° to 90°, all cases where the true edge and the reflected edge form angles less than 180° were generated. Then, the Gabor wavelet method was applied to each synthesized image (See example in **Figure S6**). The simulation result for various Gabor wavelet parameters can be found in **Figure 5B**. We noticed that when the reflected edge was perpendicular to the true edge ($\alpha = 0$), the error caused by reflection was minimized. Also, due to the flat trend around 0, cases near $\alpha = 0$ can be assumed to have minimal error.

Such analysis provided reason for implementing the background color mask and the drop profile color mask. It also explained how the masks help overcome the limitation of the naive Gabor wavelet approach. Using masks to emulate a reflected edge nearly perpendicular to the true edge, we are trying normalize each case to emulate the scenario with minimal error.

3.3 Theoretical analysis on error

First of all, ϵ_α is not 0 for all α since the derivative of $R_\alpha(\theta)$ with respect to θ at 0:

$$
\begin{aligned}
R'_\alpha(0) &= -c\int_0^\infty dx \int_{x\tan\alpha}^\infty \frac{d}{d\theta} G_\theta(x,y)\Big|_{\theta=0} dy \\
&= -c\int_0^\infty dx \int_{x\tan\alpha}^\infty -\frac{y\exp\Big(-\frac{x^2+\gamma^2y^2}{2\sigma^2}\Big)\Big((\gamma^2-1)\lambda x\sin\frac{2\pi x}{\lambda}+2\pi\sigma^2\cos\frac{2\pi x}{\lambda}\Big)}{\lambda\sigma^2} dy \\
&= \frac{c\sqrt{2}\,\pi^{3/2}\sigma^3}{\lambda}\cdot\frac{\big(1+\tan^2\alpha\big)\exp-\frac{2\pi^2\sigma^2}{\lambda^2(1+\gamma^2\tan^2\alpha)}}{\big(1+\gamma^2\tan^2\alpha\big)^{3/2}}
\end{aligned}
\tag{A.9}
$$

is almost not zero. The simulation (**Figure 5B**) shows that the error ϵ_α at $\alpha = 0$, which implies that the true edge and the reflected edge are perpendicular, is the least. Thus, we were more interested in this special case. From the definition in **Equation A.6**, the Gabor wavelet response is given by

$$
R_0(\theta) = -c\int_0^\infty dx \int_0^\infty G_\theta(x,y)\,dy. \tag{A.10}
$$

In general, evaluating θ that maximizes $R_0(\theta)$ requires solving for θ such that $dR_0/d\theta = 0$, which is non-trivial. We therefore used the 2nd-order Taylor expansion of $R_0(\theta)$.

$$
R_0(\theta) = R_0(0) + R'_0(0)\cdot\theta + \frac{R''_0(0)}{2}\cdot\theta^2 + O(\theta^3) \tag{A.11}
$$

where

$$
R'_0(0) = -c\int_0^\infty dx \int_0^\infty \frac{d}{d\theta} G_\theta(x,y)\,dy = c\sqrt{2}\,\pi^{3/2}\frac{\sigma^3\exp\big(-\frac{2\pi^2\sigma^2}{\lambda^2}\big)}{\lambda}, \tag{A.12}
$$

$$
R''_0(0) = -c\int_0^\infty dx \int_0^\infty \frac{d^2}{d\theta^2} G_\theta(x,y)\,dy = -c\sqrt{2}\,\pi^{3/2}\frac{\sigma^3}{\gamma^3\lambda}. \tag{A.13}
$$

Then the error ϵ_0, which is also the optimum θ_0^*, can be written as

$$
\epsilon_0 = \theta_0^* \approx -\frac{R'_0(0)}{R''_0(0)} = \gamma^3\exp\Big(-\frac{2\pi^2\sigma^2}{\lambda^2}\Big) \tag{A.14}
$$

For the default Gabor wavelet parameters ($\sigma = 4, \lambda = 20, \gamma = 0.2$), the error is 0.00363 in radians. Although the closed-form expression of ϵ_0 is not an accurate error estimator for real-world images due to noise, it can provide guidance for designing better Gabor wavelet parameters.

4 GUI Manual – Texture Analysis

4.1 Video & Picture Tab

Load

Click the yellow 'Select File' button. In the opened window, select the video file to be analyzed and press 'Open'. Then, press the yellow 'Load' button. Once the 'Load' button is pressed, text will appear at the bottom left of the 'Contact Angle – Texture Analysis' window indicating the status of the loaded video. At first 'Busy collecting video meta-info' will appear, followed by 'Busy reading video'. Once the video is loaded into the program the words 'Ready' will appear in the bottom left corner. At this point, you can proceed to the *Preview* tab.

Preview

The preview tab allows for a visualization of each frame of the video with a corresponding frame number for reference. A slider tab is used to parse through each frame as needed. We recommend that you refer back to the preview tab for establishing the 'Baseline Frame', 'Start Frame' and 'End Frame'. These will be discussed in further detail later in this manual.

4.2 Initialization (Surface Line) Tab

Surface Line

The baseline frame selected refers to a frame where the drop corners are well defined, so that the baseline can be determined from the locations of the drop corners. For contact angles significantly less than 90°, it is recommended to choose a baseline frame that corresponds to an early point in the drop evaporation as the corners will be well defined. For contact angels greater than or near 90°, we recommend to choose a baseline frame that corresponds to a point late in the video, when the drop corners are better defined. Once the baseline frame is selected, move on the the 'Harris Corner Detector (HCD)' box. Below are examples of what could be depicted as a 'good' reference frame and a 'bad' reference frame.

A good reference frame (Left image below) is one which the drop corners are well defined so that the HCD method will stimulate a response that corresponds to such endpoints. A bad reference frame is one which the drop corners are ambiguous and would be hard to elicit a response from the HCD method (See right image below)

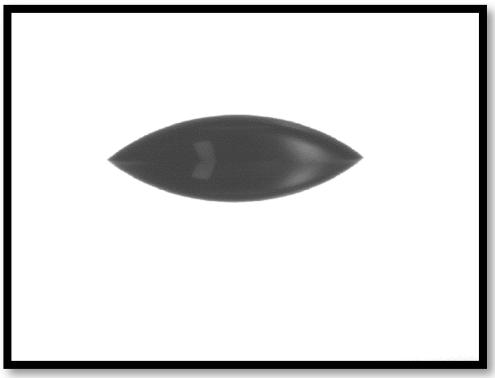

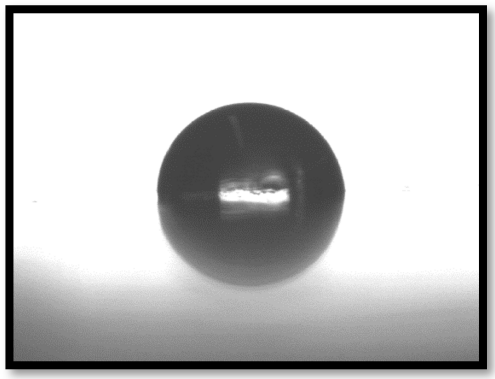

The 'Harris Corner Detector (HCD)' box allows for an adjustment on the Harris Corner Detection

variables. It is recommended that these parameters remain default.

Next, push the yellow 'Set Left' button. A window will appear displaying the selected baseline frame that was previously chosen. Using your mouse, click in the general area of the left drop corner. Once the corner is selected, press 'Enter' on your keyboard. Repeat this step with the 'Set Right' button, selecting the right corner. The standard deviation (STD) is default at 10.

Once these steps have been completed, select the yellow 'Generate' button and wait. The HCD algorithm combined with the manually selected corner points will determine the true drop corners and a surface line. A set of windows will display each step of the process. Refer to the 'Surface Line & Detected Endpoints By Edge-Xing' window to verify that the corner detection results are satisfactory. If not, re-initialize the parameters and push 'Generate'.

4.3 Initialization (Gb Filt. & Optimization) Tab

Start Frame

Using the *Preview* tab within the **Video & Picture Tab**, determine the first measurable frame of the uploaded video and set this as the 'Start frame'. Then, just as in the *Surface Line* tab, push the yellow 'Set Left' button. A window will appear displaying the selected baseline frame that was previously chosen. Using your mouse, click in the general area of the left drop corner. Once the corner is selected, press 'Enter' on your keyboard. Repeat this step with the 'Set Right' button, selecting the right corner. Refer to the display window that the corner point detection is satisfactory. If so, proceed to the *Gabor Filter* tab.

Gabor Filter

Within this tab, the parameters for 'Region of Interest' (ROI) as well as the left and right Gabor filter parameters are able to be adjusted. We recommend only adjusting the θ_l and dials. The goal of this tab is to get the left Gabor filter to match the left ROI. By match, θ_r we mean the black and white edges correspond to the black and white edges of the ROI. Attached below is a reference image. In the reference image, the 'Gabor Filter (L)' is lined up correctly according to the ROI (L), the same holds true for the right images as well.

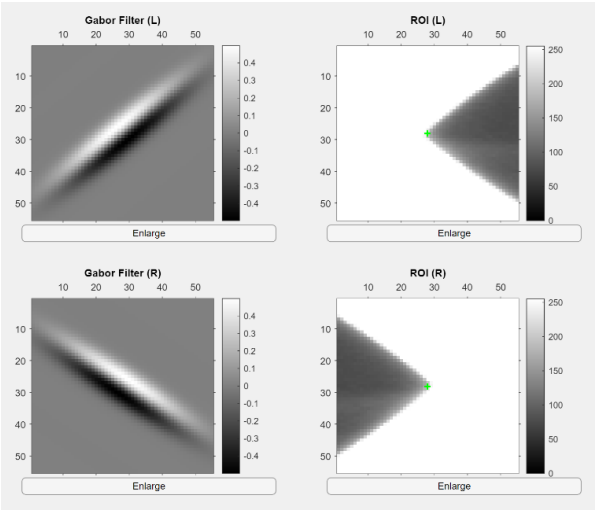

To view the adjusted Gabor filter with applied settings, click the yellow 'Set Gb Filt & View' button. Adjust the Gabor filter settings until satisfaction. Once these settings are correctly adjusted,

proceed to the *Optimization* tab.

Optimization

The first box within the *Optimization* tab is the Methods section. The methods section refers to the various methods of Gabor filter optimization. The three methods are gradient ascent, Newton's method and the mixed method. The gradient ascent and the Newton's methods will persist throughout the analysis of the video, whereas the Mixed method uses Gradient Ascent for the first frame, and Newton's for every frame after. It is recommended to choose Mixed method as that typically compensates for error in the Gabor filter initialization. The next box is titled 'Parameters (Gradient Ascent)', which controls the step size and stop criteria if using the Gradient Ascent method. The next box is identical, however for Newton's method. We recommend that regardless of the chosen method, keep these default.

The following box is titled 'ROI Pre-Processing (Background Color Mask)'. This feature will improve performance for near 90 degree cases as well as near 0 degree cases. Using an approximate RGB value of the background of the drop evaporation video, fill in the RGB values to fit the color of the background of the drop evaporation video.

The next box is titled 'Next Frame Linear Error Correction', which accounts for 'bad frames'. In some sessile drop videos, a sudden light change, etc. may produce a bad frame which could not be analyzed for the diameter or angles. So that a trial is not ruined by a single frame, the error correction tab allows for such bad frames to be skipped based upon the History length and Discard factor.

Once these parameters are set to a satisfactory level, click the white 'Set Op. & Test' button. After waiting for some time, the four frames on the right will fill in. The 'Detected Tangent (L)' and 'Detected Tangent (R)' will show the applied tangent line on the ROI. This can be used for a visual test to see if the detected tangent line is sufficient for analysis. Also, to the left two contour maps are displayed, that display the optimization routines with blue dots corresponding to the optimization output. The hope for the optimization routine is that the results (blue dots) converge to the center of the darkest red contour level. A model result of both detected tangents with the contour plots are provided below.

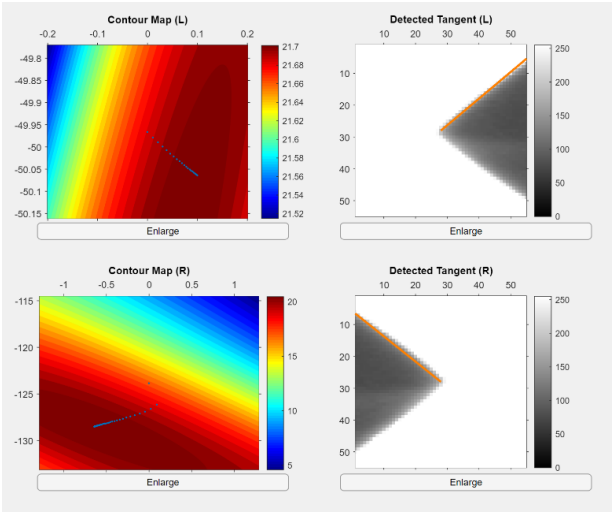

Again, as with any aspect of this program, the visualizations are provided so that you can be insured that the initialization of these complex parameters are executed correctly. If the parameters

are incorrectly applied, the visualizations will make this clear. If needed, the user always has the ability to adjust the parameters to a satisfactory level. At this point, proceed to the *Run* tab.

4.4 Run Tab

Run

In the run tab, the only adjustable parameter is the 'Frames to be proceeded' number. This refers to the last frame which the user wants to be analyzed. Again, use the *Preview* tab within the 'Video & Picture' tab to select the last frame to be analyzed. Once this is applied, click the yellow 'Run' button and proceed to the 'Result' tab.

4.5 Result Tab

Frame

This tab allows for live-tracking of the analysis procedure. A real time graph is displayed with the calculated contact angles and drop diameter for each frame. After the video is analyzed, the contents and information will be saved.